SLAC-PUB-2921
COLO-HEP-33
May 1982
(E)

RECENT RESULTS FROM MAC*

MAC Collaboration:
Colorado-Frascati-Northeastern-SLAC-Stanford-Utah-Wisconsin†
Presented by J. G. Smith, Colorado

ABSTRACT

Some preliminary results from the MAC detector at PEP are presented. These include measurements of the angular distribution of $\gamma\gamma$, $\mu\mu$, and $\tau\tau$ final states, a determination of the τ lifetime, a measurement of R, and a presentation of the inclusive muon $p_\perp$ distribution for hadronic events.

(Invited talk presented at the XVIIth Rencontre de Moriond: Workshop on New Spectroscopy, Les Arcs, France, March 20-26, 1982.)

---

*Work supported in part by the U. S. Department of Energy, under contract numbers DE-AC02-76ER02114, DE-AC03-76SF00515, and DE-AC02-76ER00881, by the National Science Foundation under contract numbers NSF-PHY77-21210, NSF-PHY77-21297, and NSF-PHY80-06504, and by I.N.F.N.

†MAC Collaborators are: W. T. Ford, J. S. Marsh, A. L. Read Jr., J. G. Smith, Department of Physics, University of Colorado, Boulder, CO 80309; A. Marini, I. Peruzzi, M. Piccolo, F. Ronga, Laboratori Nazionali Frascati dell' I.N.F.N. (Italy); L. Baksay, H. R. Band, W. L. Faissler, M. W. Gettner, G. P. Goderre, B. Gottschalk, R. B. Hurst, O. A. Meyer, J. H. Moromisato, W. D. Shambroom, E. von Goeler, R. M. Weinstein, Department of Physics, Northeastern University, Boston, MA 02115; J. V. Allaby, W. W. Ash, G. B. Chadwick, R. W. Coombes, Y. Goldschmidt-Clermont, K. H. Lau, S. P. Leung, R. L. Messner, S. J. Michalowski, K. Rich, D. E. Wiser, R. W. Zdarko, Stanford Linear Accelerator Center, Stanford, CA 94305; S. H. Clearwater, H. S. Kaye, D. M. Ritson, L. J. Rosenberg, Physics Department, Stanford University, Stanford, CA 94305; D. E. Groom, H. Y. Lee, E. C. Loh, Department of Physics, University of Utah, Salt Lake City, UT 84112; M. C. Delfino, B. K. Heltsley, J. R. Johnson, T. Maruyama, R. M. Morse, R. Prepost, Department of Physics, University of Wisconsin, Madison, WI 53706.

Introduction

The MAC (MAgnetic Calorimeter) detector consists of a central tracking detector inside a small solenoid, an electromagnetic calorimeter, scintillation counters, a segmented, toroidally magnetized steel hadron calorimeter, and large muon tracking chambers. The detector was designed to have nearly complete solid angle acceptance ($>0.95\cdot 4\pi$ for all processes), to provide good identification and measurement of photons, electrons and muons, and to measure as well as possible the total energy of events containing hadrons. The detector was installed in the winter of 1979/80 and first beam checkout began when PEP turned on in spring 1980. The data presented here were accumulated primarily during February-June 1981 and February-March 1982. The center of mass energy is 29 GeV and the useable integrated luminosity is approximately 15 pb^{-1}. Results are presented on several processes that illustrate the strengths of the MAC detector.

Detector

We give here a brief description of the detector (see Fig. 1), its resolution, calibration and triggering, since the details are described elsewhere.[1)]

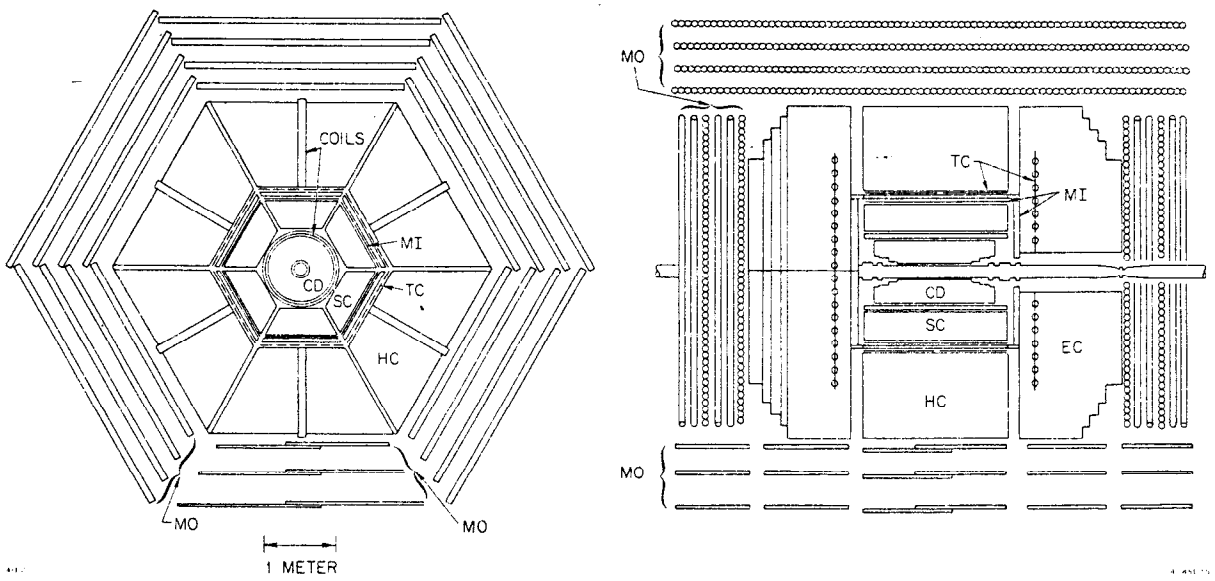

Fig. 1. MAC detector layout. The components labelled in the figure are: central drift chamber (CD), shower chamber (SC), trigger/timing scintillators (TC), central and endcap hadron calorimeters (HC, EC), and the inner and outer muon drift chambers (MI, MO). Also indicated are the solenoid and toroid coils.

Charged particle tracking is provided by a cylindrical drift chamber (CD) with ten layers of wires (four axial and six stereo layers at ±3°) surrounded by a solenoid coil giving a magnetic field of 0.57 T. The setting error of 200 μm leads to a momentum resolution $\Delta p/p \simeq .065\cdot p\cdot \sin\theta$. An electromagnetic shower counter (SC) surrounding the solenoid consists of proportional wire chambers sampling the shower which develops in 32 lead plates, each 0.5 radiation length thick. Wire groups are combined to give 192 separate azimuthal signals in each of three layers in depth. The axial position of the shower is measured using

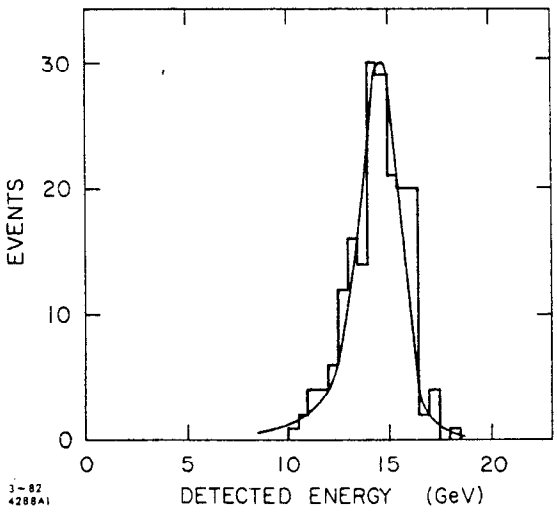

Fig. 2. Energy response of the central shower chamber to 14.5-GeV electrons. The curve is the predicted resolution function.

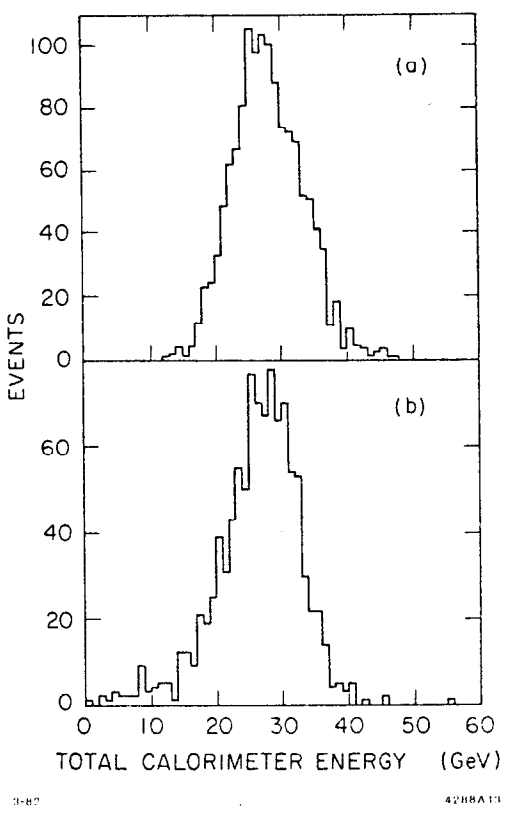

Fig. 3. Total energy for non-polar multihadron events: (a) data; (b) Monte Carlo calculation.

current division with an accuracy ≈ 2cm (1% of the length of the wires). Fig. 2 shows the energy distribution for a sample of Bhabha events. The data and Monte Carlo calculation (smooth curve) are in good agreement ($\sigma_E/E \simeq 0.08$) when the effects of 5% non-functioning channels are included. More recent data with many of these channels fixed shows the expected improved energy resolution.

A total of 144 scintillation counters (TC) inserted between the electromagnetic and hadronic calorimeters in both the central and endcap regions are used for triggering and to reject cosmic ray background. The central hadron calorimeter (HC) consists of proportional chambers interspersed between 2.5 cm steel plates totaling 5.0 absorption lengths. The readout and segmentation are the same as for the shower chambers. The endcap (EC) regions of the calorimeter also consist of proportional chambers and 6.0 absorption lengths of 2.5 cm steel plates. The anode wires in the proportional chambers are oriented to measure the radial position of a shower, while wedge-shaped cathode strips measure ϕ. Fig. 3a shows the distribution of total calorimeter energy for a sample of multihadron events for which the thrust axis satisfies $|\cos\theta| < 0.8$ (avoiding the poles of the detector where energy is not sampled). Fig. 3b shows the results of a Monte Carlo simulation using EGS[2] and HETC[3] for electromagnetic and hadronic shower development and the Lund Monte Carlo[4] for multihadron physics input. The simulation includes a realistic model of the detector geometry and shows reasonable agreement with the data energy resolution, $\sigma_E/E \simeq 0.18$.

Muon tracking drift chambers (MO) surround the entire calorimeter and additional layers (MI) are placed before the HC. The inner drift chambers are planar and the outer chambers are 10 cm diameter drift tubes. As nearly as possible given the hexagonal geometry, all wires are oriented perpendicular to the direction of bend of particles emerging from the toroidally magnetized steel. The combination of inner and outer drift

chambers measure the bend angle of muons with a multiple scattering limited precision $\Delta p/p \simeq 0.25$.

The trigger for the experiment consists of the logical OR of: (1) scintillator opposite sextants or end quadrants; (2) scintillator hits on any 3 or more of the 8 faces of the detector (modeled as a hexagonal prism with ends); (3) showers of at least 2 GeV in any 2 of: 6 SC sextants, 2 endcaps, or any part of the HC; (4) one or more penetrating tracks, defined by a string of central drift hits within a 20° sector, a hit in the corresponding scintillators, and the corresponding central hadron calorimeter sextant registering at least 400 MeV.

$e^+e^- \to \gamma\gamma$

Since PEP has run almost entirely at a single center of mass energy, 29 GeV, the reaction $e^+e^- \to \gamma\gamma$ provides the only test of QED with point-like leptons. This is because there is no lowest order weak contribution to this process. A modification to the electron propagator in this process can be parameterized by

$$\frac{d\sigma}{d\Omega} = \frac{d\sigma_0}{d\Omega}\left\{1 \pm \frac{s^2 \sin^2\theta}{2\Lambda_\pm^4}\right\} \qquad (1)$$

where

$$\frac{d\sigma_0}{d\Omega} = \frac{\alpha^2}{s}\left\{\frac{1+\cos^2\theta}{\sin^2\theta}\right\}$$

is the lowest order QED differential cross section. The inverse of Λ_+ and Λ_- can be interpreted as limits on the size of the electron. Alternatively this analysis can be interpreted as a search for a hypothetical heavy electron E*, with charge e*, in which case we set a limit on the mass of the E* with $\Lambda_+ = m_{E^*}\sqrt{e/e^*}$.

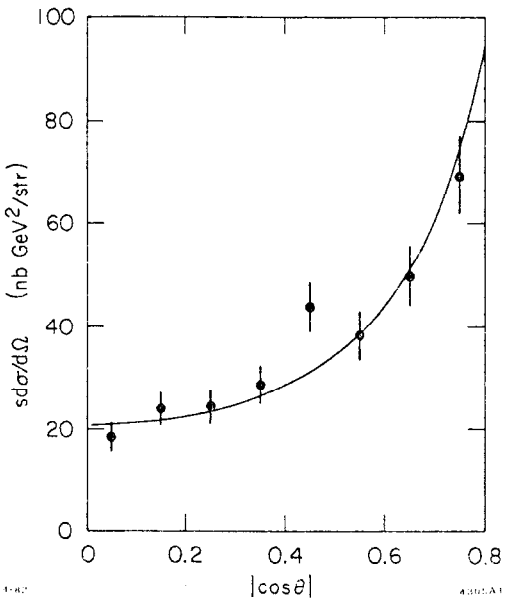

Fig. 4. Angular distribution for ee→γγ events with expected QED curve.

At present, this analysis has been performed on only 25% of the total data sample. The events are collected via the total-energy portion of the hardware trigger. The event selection requires that: at least two opposite sextants of the detector have greater than 1.5 GeV deposited in the electromagnetic portion of the calorimeter, while the remaining sextants have less than 1.5 GeV deposited energy; the total electromagnetic calorimeter energy is greater than one-half of the total center of mass energy; fewer than 10 hits are found in the central drift chamber. Corrections are made for triggering and analysis inefficiencies such as the conversion of photons in the material before the drift chamber. The data are compared to a Monte Carlo simulation which includes first order radiative corrections.[5] Fig. 4 shows the differential cross sections for the data and the Monte Carlo

calculation. A χ^2 fit to the parameterization of equation (1) has been performed in order to extract limits on the Λ parameters. Our limits at the 95% confidence level together with previous results[6),7)] are summarized in Table I.

Table I Summary of $\Lambda_\pm$ parameters for $e^+e^- \to \gamma\gamma$

	Λ_+(GeV)	Λ_-(GeV)
MAC	46	37
CELLO	43	48
JADE	47	44
MARK J	55	38
MARK II	50	41
PLUTO	46	
TASSO	34	42

$e^+e^- \to \mu^+\mu^-$ and $e^+e^- \to \tau^+\tau^-$

The differential cross section for pair production of quarks or leptons is expected to be modified by the contribution of a diagram involving the exchange of a neutral weak boson Z^0. In general it is possible that more than one such neutral vector boson could exist. We will present results here for the pair production of muons and taus. (Results for the Bhabha process have been presented previously[7)]). Ignoring lepton masses, the differential cross section for these two processes to lowest order in the weak coupling constant g can be written as

$$\frac{d\sigma}{d\Omega} = \frac{d\sigma_0}{d\Omega}\left\{ 1 - 8\, s\, g\, g_V^2 \left\{ \frac{M_Z^2}{M_Z^2 - s} \right\} - 16\, s\, g\, g_A^2 \left\{ \frac{M_Z^2}{M_Z^2 - s} \right\} \frac{\cos\theta}{1 + \cos^2\theta} \right\} \qquad (2)$$

where

$$\frac{d\sigma_0}{d\Omega} = \frac{\alpha^2}{4s}\,(1 + \cos^2\theta) \quad ,$$

g_V and g_A are the vector and axial-vector couplings of the Z^0 to charged leptons, and $g = 4.5 \times 10^{-5}\ \mathrm{GeV}^{-2}$. The second term in the above expression just alters the total cross section and is very small in the standard model but the third term modifies the angular distribution and leads to a forward-backward asymmetry defined by

$$A(\theta) = \frac{d\sigma/d\Omega(\theta) - d\sigma/d\Omega(\pi-\theta)}{d\sigma/d\Omega(\theta) + d\sigma/d\Omega(\pi-\theta)} \qquad (3)$$

with θ the angle between the outgoing lepton of the same charge as the incoming electron and $0° < \theta < 90°$. The standard model predicts a total asymmetry of -6.3% for E_{CM}=29 GeV and the nearly 4π acceptance of MAC.

The event selection for the present $\mu\mu$ analysis uses the central drift chamber rather than muon chambers for momentum measurement and requires:

1) two tracks with opposite charge, an acceptable vertex fit, and axial position within 5 cm of the mean interaction position;

2) each track be consistent with being a muon (possibly accompanied by a nearby photon) according to the calorimeter energy deposition;
3) the two tracks to be collinear to within 10°;
4) each track be outside of a ±3° azimuthal window centered on each of the twelve cracks in the detector;
5) the total momentum of the two tracks be greater than 8 GeV/c;
6) each track have associated scintillator time-of-flight (TOF) information, the mean TOF be within 4 ns of the mean for beam associated events, and the difference between the two TOF's be less than 5 ns.

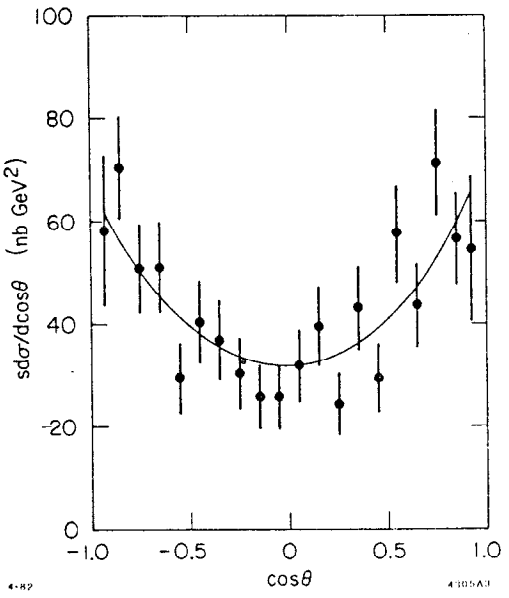

Fig. 5. Angular distribution of 846 μμ events with curve showing asymmetry best fit.

Requirements 2 and 4 reduce Bhabha contamination to an insignificant level; 1, 5, and 6 effectively eliminate cosmic ray background; and cuts 3 and 5 remove eeμμ events from the sample. The angular distribution of the 846 events in the sample is shown in Fig. 5 accompanied by the best fit curve to the form of equation 2. The data points are corrected for the asymmetry due to first order QED radiative corrections[8] which amount to 2.6% for our acceptance. Systematic errors are estimated to be less than 1%. Table II summarizes our result and the expected value for the standard model as well as the corresponding numbers for previous experiments.[7),9)] (The 34 GeV data has been used for the PETRA experiments if available). The second error if given refers to a systematic error. The large acceptance of MAC allows maximal sensitivity to the asymmetry, as evidenced by the fact that our error is comparable to the errors from the PETRA experiments which have much larger data samples.

Table II Summary of asymmetry results for μμ data

	Best fit $A_{\mu\mu}$(%)	Standard model $A_{\mu\mu}$(%)
MAC	-1.8 ± 3.3	-6.3
CELLO	-6.4 ± 6.4	-9.1
JADE	-12.8 ± 3.8 ± 1.0	-9.1
MARK J	-8.4 ± 2.9 ± 1.1	-9.5
MARK II	-6.0 ± 4.0	-6.3
PLUTO	+7 ±10	-5.8 (≃28 GeV)
TASSO	-16.1 ± 3.2	-9.3

The data sample for the ττ asymmetry analysis consists of charged 2-prong events for which the event selection is described below, and the charged 4- and 6-prong events used in the τ lifetime analysis. We reject events classified as ee or μμ and requirements 1, 4, and 6 of the μμ analysis are also used for the ττ 2-prong sample; in addition we require that:

1) the total momentum of the two tracks be greater than 2.5 GeV/c;
2) the total electromagnetic calorimeter energy be less than 20 GeV;
3) the two tracks be collinear within 50 degrees;

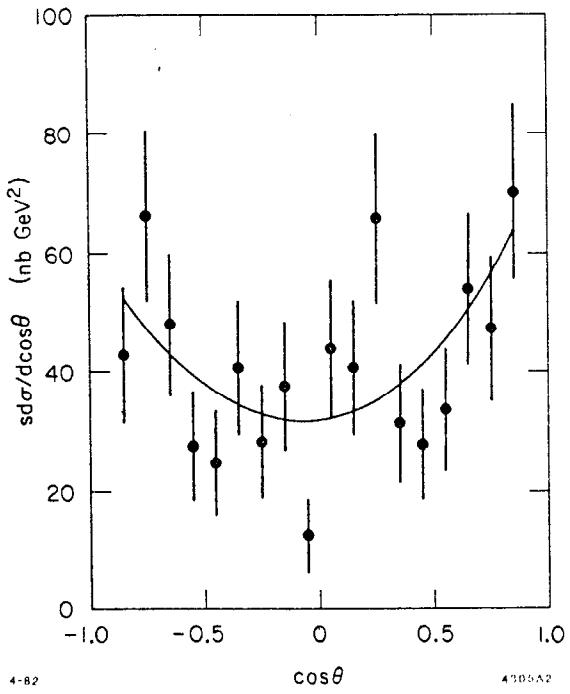

Fig. 6. Angular distribution of 242 $\tau\tau$ events with best fit curve.

4) events identified as "μe" have a $p_\perp < 1.5$ GeV/c relative to the axis for which the $p_\perp$ for the two particles is equal.

Requirement 2 is necessary in order to eliminate Bhabha events while 1, 3, 4 are necessary to reduce ee$\mu\mu$ and ee$\tau\tau$ background to a negligible level. Fig. 6 shows the angular distribution for 242 events from approximately 50% of the total data sample as well as the curve for the asymmetry best χ^2 fit. Radiative corrections are handled as in the $\mu\mu$ analysis. The results of this analysis as well as the $\tau\tau$ results from other experiments[7),10)] are summarized in Table III.

Table III Summary of asymmetry results for $\tau\tau$ data

	Best fit $A_{\tau\tau}$(%)	Standard model $A_{\tau\tau}$(%)
MAC	+3.8 ± 6.4	-6.3
CELLO	-9.3 ± 5.2	-9.2
JADE	-4.7 ± 4.2 ± 1.2	-7.5
MARK J	-7.0 ± 7.2 ± 2.1	-9.5
MARK II	-3.5 ± 5.0	-6.3
TASSO	-0.4 ± 6.6	-9.1

τ lifetime

A measurement of the lifetime of short-lived particles is possible with the MAC detector due to the good vertex position resolution of the central drift chamber afforded by its small size. We present results for the lifetime of the τ lepton extracted from a sample of events with between four and six reconstructed charged tracks. The method is to measure the transverse distance between the interaction point and the vertex position of accepted 3-prong τ decays. A sufficiently large number of such decays allows the mean of the decay path to be determined with an accuracy much better than the vertex position resolution.

The final sample of 135 events (139 3-prong τ decays) was selected by requiring:

1) the event be consistent with ee$\rightarrow\tau\tau$, with zero total charge and at least one of the τ's decaying to three charged particles;
2) the total calorimeter energy be less than the pure-electromagnetic equivalent of 24 GeV;
3) the charged-track sphericity be less than 0.03;
4) the magnitude of the total momentum of each 3-prong be greater than 4 GeV/c;
5) the larger of the two jet invariant masses determined from the calorimeter energies be less than 4.5 GeV;

6) 3-prong vertex quality cuts:
   a) an average of at least 7 hits per track;
   b) $\chi^2 < 15$ for the vertex fit (3 degrees of freedom);
   c) net charge equal to ± 1;
   d) the error on the decay length less than 8 mm.

Requirement 2 was necessary to eliminate radiative Bhabha events with the photon converting in the material before the drift chamber, though the majority of events of this type were eliminated by reconstructing the e^+e^- pairs. The contamination of $ee\tau\tau$ events in the sample was reduced to an estimated 1 event using cuts 3 and 4. Multihadron events were another important source of background, but are reduced to an estimated 7 events using requirement 5; the effect of this cut for multihadron events and the events in the present sample is shown in Fig. 7. Requirement 6 was used to remove poorly measured triplets which would have otherwise increased the systematic errors. As an example of a typical kinematic distribution, the summed magnitude of the momenta of the charged tracks is shown in Fig. 8 with a comparison curve from a Monte Carlo simulation. We find good agreement between the data and Monte Carlo for a variety of such kinematic quantities, reinforcing the conclusion that the contamination from other processes in the final sample is small.

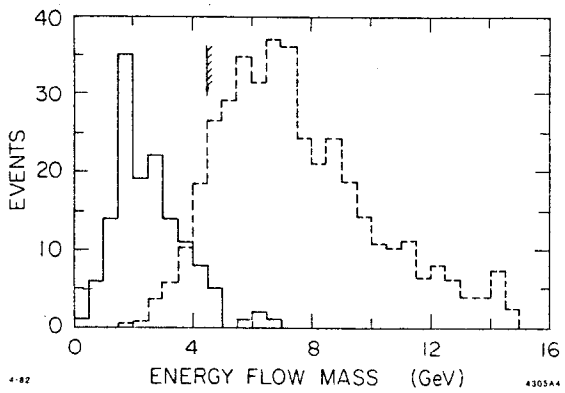

Fig. 7. Distribution of the larger of the two jet invariant masses with the cut used in the analysis shown. Solid curve: τ lifetime sample. Dashed curve: multihadron events (arbitrarily normalized).

The decay path is calculated using the displacement of the vertex transverse to the beam, correcting for the polar angle of the triplet. The uncertainty in the transverse position of the beam is $\simeq 0.7$ mm, much smaller than the typical vertex error of $\simeq 4$ mm. Fig. 9 shows the distribution for the total error in the decay length. The actual decay path distribution is shown in Fig. 10. The curve is the Monte Carlo calculated distribution using our measured lifetime.

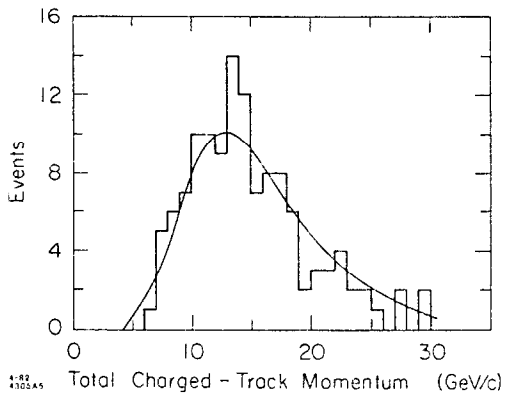

Fig. 8. Total |p| of charged tracks for τ lifetime sample with Monte Carlo curve superimposed.

In order to calculate the lifetime, we must correct the measured decay path for a bias due to the effects of finite drift chamber position resolution on the vertex fit position. We have estimated this systematic effect using a realistic simulation of the drift chamber, including non-Gaussian position errors, as well as using a sample of 3-prong vertices from multihadron data events chosen to be similar to our τ decay sample in the relevant kinematic distributions. The estimated bias in the weighted decay length from the former method is 0.55 mm, while the latter method gives 0.50 mm after correcting for the expected

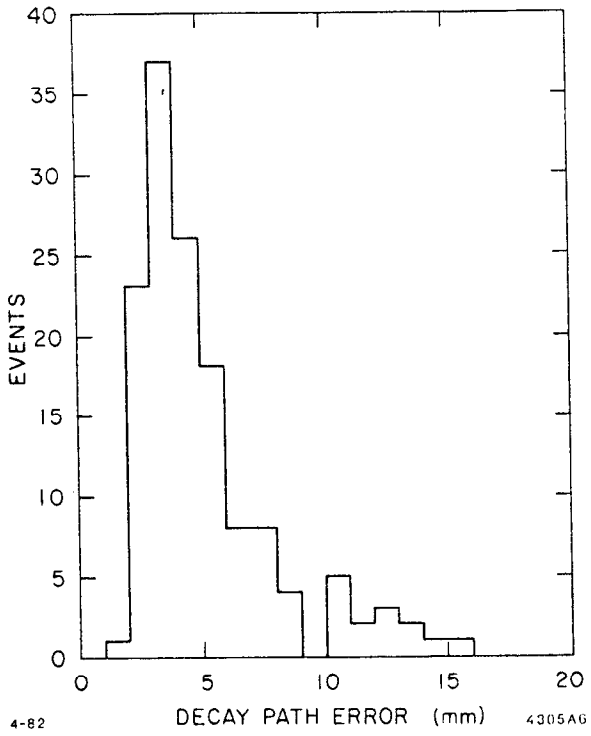

Fig. 9. Error in the decay length for τ lifetime event sample.

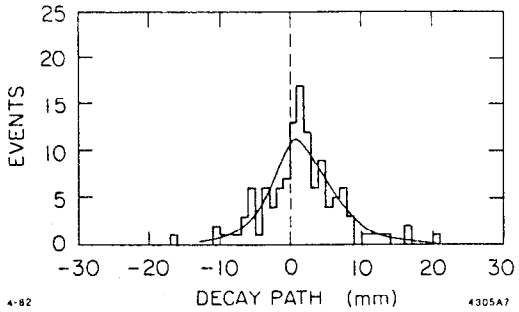

Fig. 10. Distribution of decay position for τ lifetime sample. Curve is for Monte Carlo using final measured lifetime.

bias due to short-lived hadrons in the multihadron data (0.2 mm). When the Monte Carlo estimated bias is subtracted from the weighted mean decay length for the data (1.75 ± 0.4 mm) and an estimated systematic uncertainty of 0.3 mm is added in quadrature with the statistical errors, we find

$$\tau_\tau = (4.9 \pm 2.0) \times 10^{-13} \text{ sec.}$$

The prediction assuming τ-μ universality is

$$\tau_\tau = (m_\mu/m_\tau)^5 \tau_\mu b_e = (2.8 \pm 0.2) \times 10^{-13} \text{ sec,}$$

where b_e is the branching fraction for $\tau \to e\nu\bar{\nu}$, 0.176 ± 0.016. Table IV shows our result in comparison with previous measurements of the τ lifetime[9),11)].

Table IV τ lifetime summary

	τ_τ ($\times 10^{-13}$ sec)
MAC	4.9 ± 2.0
CELLO	4.9 ± 2.9
MARK II	4.6 ± 1.9
TASSO	-0.2 ± 3.5

Hadronic cross section (R)

R, the ratio of the cross sections of ee→hadrons to ee→μμ, is expected to deviate from the simple quark model prediction (3 2/3 at PEP energies) due to gluon radiative corrections, in a way calculable with quantum chromodynamics (QCD). The first order correction term is expected to be approximately 5%. A measurement of R with sufficient accuracy would be another important test of QCD. The nearly complete solid angle acceptance and calorimetric measurement of the total hadron energy make the MAC detector well suited to a precision measurement of R.

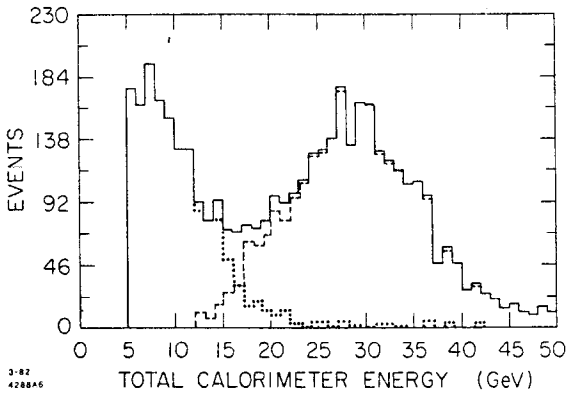

Fig. 11. Total energy for all ≥5-prong events. The dashed histogram represents events passing the selection criteria for multihadron events; events in the dotted histogram are the remainder.

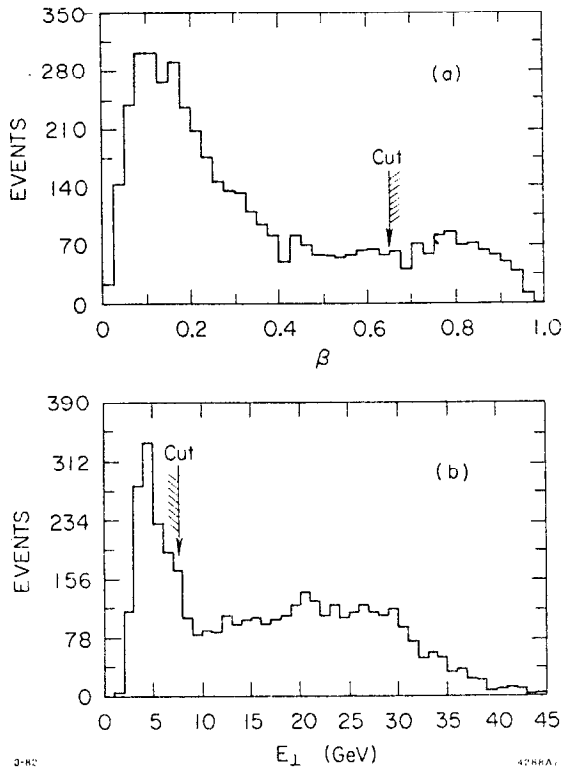

Fig. 12. (a) Imbalance and (b) $E_\perp$ distributions for all ≥5-prong events.

The primary difficulty involved in this measurement is to separate the one-photon annihilation signal from a large background dominated by two-photon annihilation. This is illustrated in Fig. 11, which shows the total energy distribution for a sample of events with at least five reconstructed tracks originating from a common vertex, consistent with coming from the interaction point. Two primary cuts are useful in eliminating the low energy two-photon background, taking advantage of the fact that these processes tend to have a relatively large net momentum along the beam direction and a small total momentum transverse to the beam. Thus we define an energy imbalance vector

$$\vec{\beta} = \sum E_i \hat{n}_i / \sum E_i,$$

and transverse energy

$$E_\perp = \sum E_i \sin\theta_i,$$

where the sums are over individual calorimeter hits with energy E_i, polar angle θ_i, and unit vector direction $\hat{n}_i$. The magnitude of the imbalance vector is plotted in Fig. 12a and $E_\perp$ in Fig. 12b for the data sample of Fig. 11. The cuts shown in the Figure, as well as several other minor cuts, result in the signal (dashed line) and background (dotted line) separation of the events in Fig. 11. In order to keep the acceptance as large as possible and thereby reduce the systematic errors due to theoretical models, no cut has been made on the polar angle of the thrust axis (see Fig. 13). However, the $E_\perp$ cut results in a loss of small polar angle events that are indistinguishable from background. Monte Carlo calculations[9] indicate that only 12% of the multihadron sample is removed by all cuts (5% if QED radiative corrections[8] are ignored), of which the $E_\perp$ cut is the most important.

A second method of multihadron analysis used the data itself to estimate the acceptance loss and background contamination of the sample. This method relies on the fact that high multiplicity, small imbalance events are nearly all one-photon signal, while events with large imbalance are largely background.

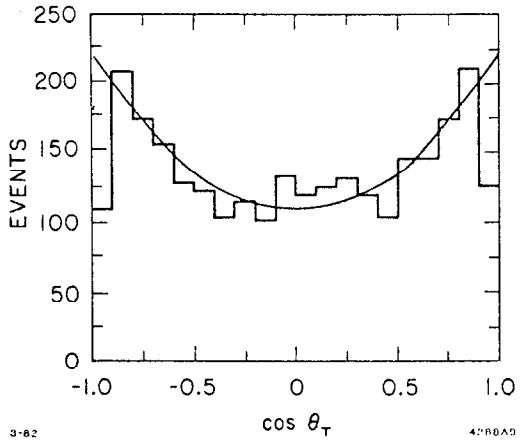

Fig. 13. Angular distribution of the thrust axis for multihadron events, determined from calorimeter energy (curve is $1 + \cos^2 \theta$).

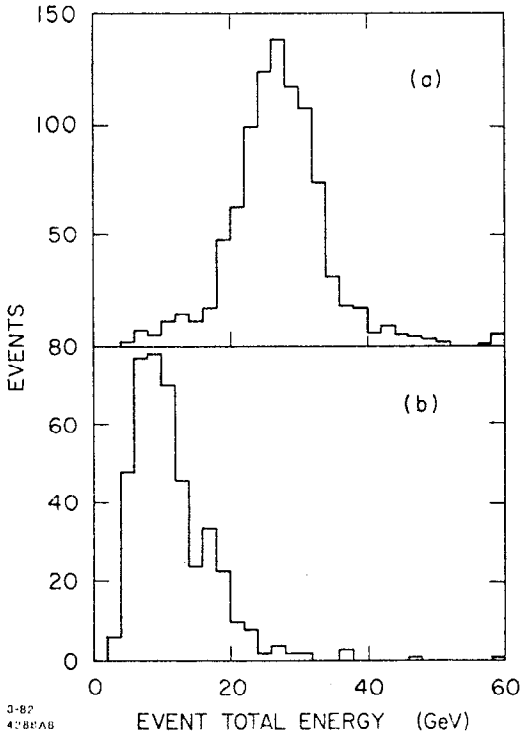

Fig. 14. (a) Events having ≥ 8 prongs and $\beta_z \leq 0.57$. (b) Events having ≥ 5 prongs and $\beta_z > 0.57$.

Fig. 14 shows the total energy distribution for these two samples, where the multiplicity cut is made at ≥ 8 charged tracks and the imbalance cut at $\beta_z = 0.57$. The shape of these distributions is then used to calculate the background leakage and signal loss due to a cut near the minimum of Fig. 11.

The results of these analyses for a sub-sample of the data representing an integrated luminosity of 5.5 pb^{-1}, give R values of 4.0 and 4.3. We estimate the total systematic error to be 7%, comprised of nearly equal contributions from event selection, luminosity measurement, and acceptance and radiative correction calculations. Thus we find

$$R = 4.1 \pm 0.05 \pm 0.3,$$

while a value of 3.9 is expected from QCD with lowest order radiative corrections and $\alpha_s = 0.17$. This result is still very preliminary and we expect the systematic errors to decrease substantially in the near future.

$e^+e^- \rightarrow \mu$ + hadrons

Multihadron events which include identified leptons can be used for a variety of interesting physics objectives, which include: (1) measurement of the lifetime of the lightest meson containing b quarks (B), thereby obtaining information on the weak mixing angles;[12] (2) measurement of a forward-backward asymmetry of large transverse momentum muons, which, for a pure b quark signal, would be expected to be a factor of three larger than the lepton pair asymmetry since the size of the asymmetry varies inversely as the parton charge; (3) measurement of the branching ratio for $B \rightarrow \mu + X$; (4) measurement of the fragmentation functions of heavy quarks; (5) search for production of new heavy quarks. Though the majority of this physics requires much larger data samples than are currently available, we give here a preliminary report on the status of our inclusive muon analysis and show our sensitivity to item (5) above.

Several features of the MAC detector are very favorable for obtaining a sample of multihadrons containing muons with low backgrounds from decay or punch-through of charged π or K mesons. The detector is compact, therefore minimizing the probability that a π or K decays before it interacts in the calorimeter. In addition, the matching of information in the central drift chamber, inner muon chambers, and outer muon chambers results in a poor χ^2 for most tracks resulting from K decays. Finally, punch-through background can be reduced to a very low level by examining the lateral spread and energy deposition of the track going through the hadron calorimeter.

A sample of multihadron events including an apparent muon was selected by requiring a visible track in the outer muon drift chambers (only those chambers covering 62% of the solid angle could be used for this analysis) correlating with a track in the hadron calorimeter which is μ-like in energy deposition and number of struck channels. Muon track information from the central and inner muon drift chambers is not yet used for this analysis. The momentum of each muon is determined by linking the outer muon chamber track with the interaction position measured by the central drift chamber, and the transverse momentum found relative to the thrust axis for the event. The $p_\perp$ distribution of 219 events from 2/3 of the total data sample is shown in Fig. 15 along with Monte Carlo calculated predictions including all known particles (solid curve) and adding a hypothetical sixth quark (dashed curve) of mass 10 GeV and charge 2/3 with a 10% branching ratio to muons. We can therefore exclude at the 95% confidence level the existence of such a new quark with a mass $m_q < 13.5$ GeV. Approximately 40% of the 50 events with $P_\perp > 1$ GeV/c are expected to result from the semileptonic decay of B mesons, while the remainder are roughly equally split between the semileptonic decays of charmed particles and background from π or K mesons.

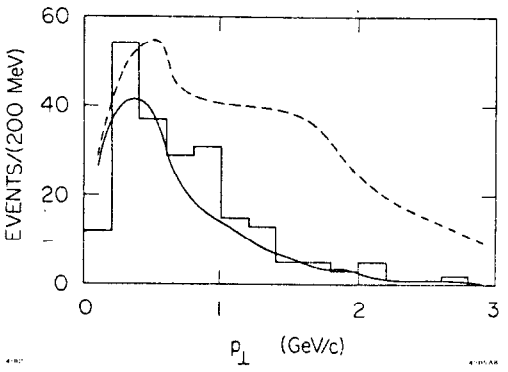

Fig. 15. Momentum perpendicular to the thrust axis for muons in multihadron events. Solid curve: calculated contribution from π, K, c, and b decay. Dashed curve: contribution including a 10-GeV t-quark with 10% muonic branching ratio.

Conclusion

We have presented limits on the Λ parameters for the process $ee \to \gamma\gamma$. The asymmetries for the processes $ee \to \mu\mu$ and $ee \to \tau\tau$ are measured as a test of the electroweak theories. The lifetime of the τ lepton has been measured and is in general agreement with the expected value. The ratio R has been measured with a systematic uncertainty of 7% with considerable improvement anticipated soon. Finally, the $p_\perp$ distribution for a sample of $ee \to \mu + X$ events was shown to be in agreement with expectations from currently known quarks.

Acknowledgements

I would like to thank the conference organizers, in particular J. Trân Thanh Vân and J. F. Grivaz, for their help and for contributing to make this conference the most enjoyable I have ever attended.

References

1. MAC Collaboration, in Proceedings of the International Conference on Instrumentation for Colliding Beams, edited by W. Ash (SLAC, 1982), to be published; SLAC-2894.

2. R. L. Ford and W. R. Nelson, SLAC-210 (1978), unpublished.

3. T. A. Gabriel and B. L. Bishop, Nucl. Instr. and Methods 155, 81 (1978), and references therein.

4. T. Sjöstrand, LUND LU TP 80-3 (1980).

5. F. A. Berends and R. Kleiss, Nucl. Phys. B186, 72 (1981).

6. G. Wolf, DESY 81-086 (1981).

7. R. Hollebeek, in Proceedings of the 1981 International Symposium on Lepton and Photon Interactions at High Energies, Bonn, Edited by W. Pfeil (Physicalisches Institut, University of Bonn,1981), p.1.

8. F. A. Berends and R. Kleiss, Nucl. Phys. B177, 237 (1981).

9. P. Steffen, proceedings of this conference.

10. J. Strait, proceedings of this conference.

11. G. J. Feldman, et al., Phys. Rev. Letters 56, 66 (1982).

12. H. Harari, SLAC-2234 (1978), unpublished.
B. D. Gaiser, T. Tsao, and M. B. Wise, Annals of Physics 132, 66 (1981).
M. K. Gaillard and L. Maiani, Proceedings of the Cargese Summer Institute, 433 (1979).